

New magnetic field measurements of β Cephei stars and slowly pulsating B stars*

S. Hubrig^{1,2,**}, M. Briquet³, P. De Cat⁴, M. Schöller⁵, T. Morel⁶, and I. Ilyin²

¹ European Southern Observatory, Casilla 19001, Santiago 19, Chile

² Astrophysikalisches Institut Potsdam, An der Sternwarte 16, D-14482 Potsdam, Germany

³ Instituut voor Sterrenkunde, Katholieke Universiteit Leuven, Celestijnenlaan 200B, B-3001 Leuven, Belgium

⁴ Koninklijke Sterrenwacht van België, Ringlaan 3, B-1180 Brussel, Belgium

⁵ European Southern Observatory, Karl-Schwarzschild-Str. 2, D-85748 Garching bei München, Germany

⁶ Institut d'Astrophysique et de Géophysique, Université de Liège, Allée du 6 Août, Bât. B5c, 4000 Liège, Belgium

Received 2008 Dec 10, accepted 2009 Jan 12

Published online 2009 Apr 17

Key words stars: early types – stars: fundamental parameters – stars: individual (δ Cet, ξ^1 CMa, 15 CMa, V1449 Aql, 53 Psc, CG Hyi, 33 Eri, 40 Tau, V1143 Tau, V1144 Tau, γ Col, HY Vel, V335 Vel, V847 Ara, V1070 Sco, V1092 Sco, α Tel, V338 Sge, V4199 Sgr, V4372 Sgr, DK Oct, 21 CMa, HR 6320) – stars: magnetic fields – stars: oscillations

We present the results of the continuation of our magnetic survey with FORS 1 at the VLT of a sample of B-type stars consisting of confirmed or candidate β Cephei stars and Slowly Pulsating B (hereafter SPB) stars, along with a small number of normal B-type stars. A weak mean longitudinal magnetic field of the order of a few hundred Gauss was detected in three β Cephei stars and two stars suspected to be β Cephei stars, in five SPB stars and eight stars suspected to be SPB stars. Additionally, a longitudinal magnetic field at a level larger than 3σ has been diagnosed in two normal B-type stars, the nitrogen-rich early B-type star HD 52089 and in the B5 IV star HD 153716. Roughly one third of β Cephei stars have detected magnetic fields: Out of 13 β Cephei stars studied to date with FORS 1, four stars possess weak magnetic fields, and out of the sample of six suspected β Cephei stars two show a weak magnetic field. The fraction of magnetic SPBs and candidate SPBs is found to be higher: Roughly half of the 34 SPB stars have been found to be magnetic and among the 16 candidate SPBs eight stars possess magnetic fields. In an attempt to understand why only a fraction of pulsating stars exhibit magnetic fields, we studied the position of magnetic and non-magnetic pulsating stars in the H-R diagram. We find that their domains in the H-R diagram largely overlap, and no clear picture emerges as to the possible evolution of the magnetic field across the main sequence. It is possible that stronger fields tend to be found in stars with lower pulsating frequencies and smaller pulsating amplitudes. A somewhat similar trend is found if we consider a correlation between the field strength and the $v \sin i$ -values, i.e. stronger magnetic fields tend to be found in more slowly rotating stars.

© 2009 WILEY-VCH Verlag GmbH & Co. KGaA, Weinheim

1 Introduction

We started our systematic search for magnetic fields in pulsating B-type stars after the detection of a weak magnetic field in two β Cephei stars, in the prototype of the class, β Cep itself, by Henrichs et al. (2000) and in V2052 Oph by Neiner et al. (2003a). The first detection of a weak magnetic field in the SPB star ζ Cas was reported by Neiner et al. (2003b). In our first publication on the magnetic survey of pulsating B-type stars (Hubrig et al. 2006), we announced detections of weak mean longitudinal magnetic fields of the order of a few hundred Gauss in 13 SPB stars and in the β Cephei star ξ^1 CMa. Among the three β Cephei stars with detected magnetic fields, ξ^1 CMa showed the largest mean longitudinal field of the order of 300 G.

However, the role of magnetic fields in modeling oscillations of B-type stars remains to be studied. Our previous

search for correlations between the strength of the magnetic field and stellar fundamental parameters, using available, rather scarce data, was unsuccessful. We also did not find any hint of relations between the magnetic field strength and other stellar parameters. The position of the magnetic pulsating stars in the H-R diagram did not indicate a noticeable difference in the evolutionary stage between the non-magnetic and magnetic pulsating stars. On the other hand, the whole sample under previous study contained only 14 stars with detected magnetic fields. Clearly, to obtain better statistics it is necessary to increase the sample of targets with magnetic field measurements. The aim of the current study is to analyse β Cep and SPBs as a group, such as the distributions of their magnetic fields and their relation to stellar fundamental parameters, that is stellar mass, effective temperature, projected rotation velocity, evolutionary state in terms of elapsed fraction of main-sequence lifetime, and pulsation period. Magnetic field measurements have been collected with FORS 1 at the VLT in the last two years. With this new dataset and the previous dataset presented

* Based on observations obtained at the European Southern Observatory, Paranal, Chile (ESO programmes 078.D-0140(A), 078.D-0330(A), 079.D-0241(A), and 080.D-0383(A)).

** Corresponding author: shubrig@aip.de

by Hubrig et al. (2006), we now obtained at least one measurement for each of the currently confirmed 34 SPB stars visible from the Southern hemisphere and for 13 β Cephei stars. The SPB-like variability of most of the studied SPBs was discovered by the Hipparcos satellite (Waelkens et al. 1998). Their membership in the SPB class has been confirmed by long-term photometric and spectroscopic monitoring projects undertaken by members of the Institute of Astronomy of the University of Leuven. We refer to De Cat (2007) for a recent review on SPB stars.

Here we present the results of 98 magnetic field measurements in a sample of 60 stars, which includes confirmed and suspected β Cephei and SPB stars and a small fraction of early to mid normal B-type stars. We describe the derivation of the fundamental parameters of the stars in our sample and discuss the occurrence and strength of their magnetic fields in the context of their position in the H-R diagram.

2 The sample of pulsating stars

Besides the confirmed SPB stars studied by long-term photometric and spectroscopic monitoring projects, we enlarged our magnetic field search to several other Hipparcos SPB stars. In the Hipparcos lightcurves, these targets show periods of the order of days, which correspond to the pulsation range of SPB stars. Furthermore, all these stars have been found to be located in the SPB instability strip. Currently, we consider them as suspected SPB or candidate SPB stars since additional studies of their variability are needed to definitely conclude on their nature. Many chemically peculiar B-type magnetic stars, so-called Bp stars and ellipsoidal variables are also found in the same part of the H-R diagram. For these stellar types the observed variations are operating on similar timescales, but are usually attributed to rotation or binarity, instead of pulsations (Briquet et al. 2001, 2004).

The further goal of the present study was to enlarge the number of magnetic field measurements for a sample of β Cephei stars. Among them, the β Cephei stars δ Cet and ξ^1 CMa were selected for monitoring because of the similarity of their pulsation behaviour. ξ^1 CMa was re-observed a couple of times with the aim to investigate its magnetic variability. As we mentioned in our previous work (Hubrig et al. 2006), δ Cet and three β Cephei stars with detected magnetic fields, V2052 Oph, ξ^1 CMa and β Cep, share common properties: all four are nitrogen enriched (Morel et al. 2006), and all of them are either radial pulsators (ξ^1 CMa) or their multiperiodic pulsations are dominated by a radial mode (δ Cet, β Cep, and V2052 Oph). The presence of a magnetic field in these stars might play an important role to explain these physical characteristics. To search for the presence of possible differences in fundamental parameters between pulsating and non-pulsating stars we also selected seven non-pulsating normal early to mid B-type stars including the nitrogen-rich B star HD 52089 recently studied by Morel et al. (2008).

All stars are very bright ($V \leq 8$) and their pulsational behaviour has been intensively studied during the last years. The fundamental parameters of the studied β Cephei stars (both confirmed and suspected) are presented in Table 1a, those of SPB and candidate SPB stars in Table 1b, and Table 1c contains the fundamental parameters of normal B-type stars and the N-rich star HD 52089.

For all the objects in our sample, observations in the GENEVA photometric system are available. Mean GENEVA magnitudes were used to obtain the effective temperature T_{eff} and the surface gravity $\log g$ with the method described by Künzli et al. (1997) (Cols. 4 and 5 in Tables 1a–1c). In Table 1a the T_{eff} and $\log g$ values of HD 44743, ξ^1 CMa, HD 50707, HD 129557, and HD 180642 are inaccurate because an extrapolation outside the calibration grid was needed for their determination. The same extrapolation was used for HD 52089 in Table 1c. All these values are set in *italics*. To derive other stellar parameters, a grid of main-sequence models has been used, which was calculated with the Code Liégeois d'Évolution Stellaire (version 18.2, Scuflaire et al. 2008), assuming solar composition. For a detailed description see “grid 2” in De Cat et al. (2006). The mass M , the radius R , the luminosity $\log(L/L_{\odot})$, and the age of the star expressed as a fraction of its total main-sequence lifetime f are presented in Cols. 6 to 9 in Tables 1a–1c. We note that the SIMBAD spectral classification as giants or supergiants of a number of β Cephei and SPB stars is in all cases misleading, probably due to the low $v \sin i$ values of the considered stars. The fundamental parameters presented in Tables 1a–1c clearly show that only one star in our sample, HD 40494, is in an advanced evolutionary state, just behind the terminal-age main sequence (TAMS).

For almost all studied stars numerous spectroscopic observations have been obtained in previous years at the ESO La Silla observatory and Observatoire de Haute-Provence (Aerts et al. 1998; Mathias et al. 2001; Uytterhoeven et al. 2001; De Cat & Aerts 2002; Aerts et al. 2004a, 2004b). To estimate the projected rotational velocity $v \sin i$ (Col. 10 in Tables 1a–1c), an average of all spectra has been used for single stars. For binaries with a well-known orbit, the orbital motion was removed before averaging the spectra. In case of double-lined systems, usually the spectrum with the maximum observed separation between the components was chosen for the $v \sin i$ determination. For slowly rotating β Cephei and SPB stars we selected several unblended absorption lines: the $\lambda 4560 \text{ \AA}$ Si III-triplet and/or the $\lambda 4130 \text{ \AA}$ Si II-doublet. For rapidly rotating stars, only the $\lambda 4481 \text{ \AA}$ Mg II-line has been used. We applied the method of least squares fitting with rotationally broadened synthetic profiles using a Gaussian intrinsic width but without taking into account pulsational broadening.

For fifteen stars we do not have high-resolution spectroscopic observations. For thirteen stars it was possible to gather $v \sin i$ values from the literature. The $v \sin i$ values for HD 27742, HD 40494, HD 61068, HD 129557,

Table 1a The observed β Cephei stars. In the first three columns we list the HD number, another identifier, the spectral type retrieved from the SIMBAD database and membership in a spectroscopic binary system. An asterisk in front of the HD number denotes candidate β Cephei stars. The effective temperature T_{eff} and the surface gravity $\log g$ are listed in Cols. 4 and 5 (see text). In Cols. 6 to 10 we present the stellar mass M , the radius R , the luminosity $\log(L/L_{\odot})$ and the age of the star expressed as a fraction of its total main-sequence lifetime f . The last column gives $v \sin i$ -values.

HD	Other Identifier	Spectral Type	T_{eff} [10^3 K]	$\log g$	M/M_{\odot}	R/R_{\odot}	$\log(L/L_{\odot})$	f [%]	$v \sin i$ [km s^{-1}]
16582	δ Cet	B2 IV	21.9 \pm 1.0	4.05 \pm 0.20	8.4 \pm 0.7	4.6 \pm 0.8	3.6 \pm 0.2	58 \pm 21	7 \pm 4
29248	ν Eri	B2 III	23.0 \pm 1.1	3.92 \pm 0.20	10.1 \pm 0.8	6.1 \pm 0.9	4.0 \pm 0.1	79 \pm 13	21 \pm 12
44743	β CMa	B1 II-III	26.4 \pm 1.2	3.79 \pm 0.20	13.5 \pm 1.0	7.5 \pm 1.1	4.4 \pm 0.1	82 \pm 9	11 \pm 7
46328	ξ^1 CMa	B1 III	27.1 \pm 1.2	3.83 \pm 0.20	13.7 \pm 0.9	7.1 \pm 0.9	4.4 \pm 0.1	76 \pm 10	20 \pm 7
50707	15 CMa	B1 Ib	26.1 \pm 1.2	3.89 \pm 0.20	12.8 \pm 1.2	6.8 \pm 1.2	4.3 \pm 0.2	75 \pm 13	20 \pm 12
* 55958	GG CMa	B2 IV	19.2 \pm 0.9	4.15 \pm 0.20	6.4 \pm 0.4	3.6 \pm 0.5	3.2 \pm 0.1	45 \pm 23	—
61068	PT Pup	B2 II	23.8 \pm 1.1	4.01 \pm 0.20	10.1 \pm 0.8	5.4 \pm 0.9	3.9 \pm 0.2	64 \pm 18	10 \pm 9
* 74575	α Pyx	B1.5 III	23.8 \pm 1.1	3.89 \pm 0.20	10.7 \pm 0.9	6.3 \pm 1.0	4.0 \pm 0.1	79 \pm 12	11 \pm 2
111123	β Cru	B0.5 III, SB1	27.3 \pm 1.3	3.73 \pm 0.20	14.1 \pm 0.7	7.5 \pm 0.7	4.4 \pm 0.1	81 \pm 6	16 \pm 9
129557	BU Cir	B2 III	24.9 \pm 1.1	4.06 \pm 0.20	10.5 \pm 0.7	5.0 \pm 0.8	3.9 \pm 0.1	51 \pm 21	53 \pm 16
129929	V836 Cen	B3 V	23.9 \pm 1.1	4.03 \pm 0.20	10.1 \pm 0.7	5.2 \pm 0.8	3.9 \pm 0.1	61 \pm 19	8 \pm 5
* 132200	κ Cen	B2 IV	19.8 \pm 0.9	4.02 \pm 0.20	7.2 \pm 0.5	4.4 \pm 0.7	3.4 \pm 0.2	64 \pm 19	11 \pm 7
* 136504	ϵ Lup	B2 IV-V, SB	19.3 \pm 0.9	3.89 \pm 0.20	7.4 \pm 0.6	5.2 \pm 0.9	3.5 \pm 0.2	83 \pm 13	41 \pm 9
* 171034	HR 6960	B2 IV-V	18.8 \pm 0.9	3.81 \pm 0.20	7.3 \pm 0.5	5.3 \pm 0.7	3.5 \pm 0.1	87 \pm 9	107 \pm 16
* 172910	HR 7029	B2.5 V	18.8 \pm 0.9	4.23 \pm 0.20	6.1 \pm 0.4	3.4 \pm 0.4	3.1 \pm 0.1	37 \pm 20	7 \pm 4
180642	V1449 Aql	B1.5 II-III	27.8 \pm 1.3	4.14 \pm 0.20	12.6 \pm 1.0	5.1 \pm 0.8	4.1 \pm 0.1	36 \pm 22	15 \pm 9

HD 136504, HD 142378, HD 169033, and HD 171034 were taken from Abt et al. (2002). For HD 23958 and HD 169820 the $v \sin i$ values were found in Royer et al. (2002). For the normal B-type star HD 24626 we used the $v \sin i$ value from Hempel & Holweger (2003) and the data from Balona (1975) were used for the other two normal B-type stars, HD 153716 and HD 166197.

3 Spectropolarimetric observations

The spectropolarimetric observations have been carried out in the years 2006 to 2008 at the European Southern Observatory with FORS 1 (FOcal Reducer low dispersion Spectrograph) mounted on the 8-m Melipal telescope of the VLT. This multi-mode instrument is equipped with polarization analyzing optics comprising super-achromatic half-wave and quarter-wave phase retarder plates, and a Wollaston prism with a beam divergence of $22''$ in standard resolution mode. For the major part of observations we used the GRISM 600B in the wavelength range 3480–5890 Å to cover all hydrogen Balmer lines from H β to the Balmer jump. The observations at the end of August–beginning of September 2007 have been carried out with a new mosaic detector with blue optimised E2V chips, which was implemented in FORS 1 at the beginning of April 2007. It has a pixel size of 15 μm (compared to 24 μm for the previous Tektronix chip) and higher efficiency in the wavelength range below 6000 Å. With the new mosaic detector and the GRISM 600B we are now also able to cover a much larger spectral range, from 3250 to 6215 Å. Two observations of δ Cet at the end of 2006 have been carried out with GRISM 600R in the wavelength range 5240–7380 Å. In all

observations a slit width of $0''.4$ was used to obtain a spectral resolving power of $R \sim 2000$ with GRISM 600B and $R \sim 3000$ with GRISM 600R. During the observing run in August/September 2007 two β Cep stars, ξ^1 CMa and δ Cet, have been observed with the GRISM 1200B covering the Balmer lines from H β to H8, and a slit width of $0''.4$ to obtain a spectral resolving power of $R \sim 4000$.

Usually, we took four to eight continuous series of two exposures for each star in our sample with the retarder waveplate oriented at two different angles, $+45^\circ$ and -45° . All stars in our sample are bright and since the errors of the measurements of the polarization with FORS 1 are determined by photon counting statistics, a signal-to-noise ratio of a few thousands can be reached for bright stars within ~ 30 min. More details on the observing technique with FORS 1 can be found elsewhere (e.g., Hubrig et al. 2004a, 2004b). The mean longitudinal magnetic field is the average over the stellar hemisphere visible at the time of observation of the component of the magnetic field parallel to the line of sight, weighted by the local emergent spectral line intensity. It is diagnosed from the slope of a linear regression of V/I versus the quantity $-\frac{g_{\text{eff}}e}{4\pi m_e c^2} \lambda^2 \frac{dI}{d\lambda} \langle B_z \rangle + V_0/I_0$, where V is the Stokes parameter which measures the circular polarization, I is the intensity observed in unpolarized light, g_{eff} is the effective Landé factor, e is the electron charge, λ is the wavelength expressed in Å, m_e the electron mass, c the speed of light, $dI/d\lambda$ is the derivative of Stokes I , and $\langle B_z \rangle$ is the mean longitudinal field. Our experience from a study of a large sample of magnetic and non-magnetic Ap and Bp stars revealed that this regression technique is very robust and that detections with $B_z > 3\sigma$ result only for stars possessing magnetic fields.

Table 1b Same as in Table 1a for the observed SPB stars. An asterisk denotes candidate SPB stars.

HD	Other Identifier	Spectral Type	T_{eff} [10^3 K]	$\log g$	M/M_{\odot}	R/R_{\odot}	$\log(L/L_{\odot})$	f [%]	$v \sin i$ [km s^{-1}]
3379	53 Psc	B2.5I V	17.3±0.8	4.16±0.20	5.4±0.4	3.3±0.5	2.9±0.1	45±23	33±17
* 11462	CG Hyi	B8 V	12.6±0.6	4.31±0.20	3.2±0.2	2.2±0.2	2.0±0.1	31±17	23±13
* 23958	HR 1186	B8 V	12.5±0.6	4.05±0.20	3.5±0.3	3.0±0.5	2.3±0.2	65±18	320±16
24587	33 Eri	B5 V, SB1	13.9±0.6	4.26±0.20	3.7±0.2	2.5±0.3	2.3±0.1	36±19	28±1
25558	40 Tau	B3 V	16.4±0.8	4.22±0.20	4.9±0.3	3.0±0.4	2.8±0.1	39±21	14±8
26326	GU Eri	B5 IV	15.2±0.7	4.14±0.20	4.4±0.3	3.0±0.5	2.7±0.1	49±22	11±6
* 26739	GY Eri	B5 IV	15.3±0.7	4.09±0.20	4.6±0.3	3.3±0.5	2.7±0.1	57±21	16±8
* 27742	V1141 Tau	B8 IV-V	12.7±0.6	4.13±0.20	3.4±0.2	2.7±0.4	2.2±0.1	53±21	175±24
28114	V1143 Tau	B6 IV	14.6±0.7	4.00±0.20	4.5±0.3	3.5±0.6	2.7±0.2	72±17	9±5
28475	V1144 Tau	B5 V	15.1±0.7	3.97±0.20	4.8±0.4	3.8±0.6	2.8±0.2	76±15	15±8
* 29376	V1148 Tau	B3 V, SB	16.5±0.8	4.19±0.20	5.0±0.3	3.1±0.4	2.8±0.1	42±22	89±15
* 33331	TU Pic	B5 III	13.0±0.6	4.22±0.20	3.4±0.2	2.5±0.3	2.2±0.1	40±21	27±14
34798	YZ Lep	B5 IV-V, SB ?	15.6±0.7	4.25±0.20	4.5±0.3	2.8±0.3	2.6±0.1	37±20	34±2
37151	V1179 Ori	B8 V	12.9±0.6	4.34±0.20	3.3±0.2	2.2±0.2	2.1±0.1	27±15	11±6
39844	ϵ Dor	B6 V	13.7±0.6	3.89±0.20	4.3±0.3	3.8±0.6	2.7±0.1	84±11	9±5
* 40494	γ Col	B2.5 IV	15.9±0.7	3.72±0.20	5.7±0.3	4.8±0.4	3.1±0.1	93±5	96±16
45284	BD−07°1424	B8, SB2	14.7±0.7	4.40±0.20	3.9±0.2	2.4±0.2	2.4±0.1	19±11	71±6
53921	V450 Car	B9 IV, SB2	13.7±0.6	4.23±0.20	3.7±0.2	2.6±0.3	2.3±0.1	39±21	17±10
* 55718	V363 Pup	B3 V	16.1±0.7	4.17±0.20	4.8±0.3	3.1±0.5	2.8±0.1	45±23	179±4
69144	NO Vel	B2.5 IV	15.9±0.7	3.80±0.20	5.5±0.3	4.6±0.5	3.1±0.1	89±8	67±2
74195	\omicron Vel	B3 IV	16.2±0.7	3.91±0.20	5.5±0.4	4.3±0.7	3.0±0.2	82±13	9±5
74560	HY Vel	B3 IV, SB1	16.2±0.7	4.15±0.20	4.9±0.3	3.1±0.5	2.8±0.1	46±24	13±7
85953	V335 Vel	B2 III	18.4±0.8	3.91±0.20	6.8±0.6	4.9±0.8	3.4±0.2	82±13	18±10
* 128585	IS Lup	B3 IV	16.6±0.8	3.89±0.20	5.8±0.4	4.5±0.7	3.1±0.1	83±12	132±12
140873	25 Ser	B8 III, SB2	13.9±0.6	4.35±0.20	3.7±0.2	2.4±0.2	2.3±0.1	26±15	70±2
* 152511	V847 Ara	B5 III	14.8±0.7	4.23±0.20	4.2±0.3	2.7±0.4	2.5±0.1	39±21	26±15
* 152635	V1070 Sco	B7 II	13.8±0.6	4.31±0.20	3.6±0.2	2.4±0.3	2.3±0.1	30±17	5±3
* 163254	V1092 Sco	B2 IV/V	18.1±0.8	4.10±0.20	6.0±0.4	3.7±0.6	3.1±0.1	53±22	110±6
* 169467	α Tel	B3 IV	16.7±0.8	4.12±0.20	5.2±0.4	3.3±0.5	2.9±0.1	51±22	14±8
169820	BD+14°3533	B9 V	11.8±0.5	4.26±0.20	2.9±0.2	2.2±0.3	1.9±0.1	37±20	136±7
179588	V338 Sge	B9 IV	12.2±0.6	4.28±0.20	3.0±0.2	2.2±0.3	2.0±0.1	34±19	20±12
181558	V4199 Sgr	B5 III	14.7±0.7	4.16±0.20	4.2±0.3	2.9±0.5	2.5±0.1	46±23	6±4
* 183133	V4372 Sgr	B2 IV	16.7±0.8	3.99±0.20	5.5±0.4	4.0±0.7	3.0±0.2	72±17	25±13
191295	V1473 Aql	B7 III	13.1±0.6	4.14±0.20	3.6±0.2	2.7±0.4	2.3±0.1	51±22	9±6
* 205879	DK Oct	B8 V	12.5±0.6	4.23±0.20	3.2±0.2	2.4±0.3	2.1±0.1	40±21	11±6
206540	BD+10°4604	B5 IV	14.0±0.6	4.11±0.20	4.0±0.3	3.0±0.5	2.5±0.1	55±21	8±5
* 215573	ξ Oct	B6 IV	14.0±0.6	4.09±0.20	4.0±0.3	3.0±0.5	2.5±0.1	58±20	5±2

Table 1c Same as in Table 1a for the observed normal B stars and the N-rich star HD 52089.

HD	Other Identifier	Spectral Type	T_{eff} [10^3 K]	$\log g$	M/M_{\odot}	R/R_{\odot}	$\log(L/L_{\odot})$	f [%]	$v \sin i$ [km s^{-1}]
24626	i Eri	B6 V	14.1±0.6	4.24±0.20	3.8±0.2	2.6±0.4	2.4±0.1	38±20	29±2
52089	21 CMa	B2 Iab	25.1±1.2	3.82±0.20	12.5±1.3	7.3±1.3	4.3±0.2	84±10	28±2
142378	47 Lib	B2/B3 V	16.1±0.7	4.38±0.20	4.5±0.2	2.6±0.2	2.6±0.1	21±12	230±24
153716	HR 6320	B5 IV	15.5±0.7	4.07±0.20	4.7±0.3	3.4±0.5	2.8±0.1	60±20	187±10
164245	HR 6708	B7 IV	12.9±0.6	4.03±0.20	3.7±0.3	3.1±0.5	2.4±0.2	68±17	—
166197	NSV 10304	B1 V	23.8±1.1	3.75±0.20	11.5±1.1	7.2±1.1	4.2±0.1	88±7	229±15
169033	BD−12°5024	B5 V	12.0±0.6	3.82±0.20	3.6±0.2	3.6±0.4	2.4±0.1	88±8	160±24

To search for temporal variability of the magnetic field of ξ^1 CMa we planned to obtain a series of spectropolarimetric observations with the 2.56 m Nordic Optical Telescope (NOT, La Palma) using the SOFIN echelle spectrograph. However, due to bad weather conditions, only one rather noisy high resolution spectropolarimetric observation with an exposure time of 30 s and a S/N ratio of ~ 150 was obtained on 2008 September 13. SOFIN is a high-resolution echelle spectrograph mounted at the Cassegrain focus of NOT (Tuominen et al. 1999) and equipped with three optical cameras providing different resolving powers of 30 000, 80 000, and 160 000. ξ^1 CMa was observed with the low-resolution camera with $R = \lambda/\Delta\lambda \approx 30\,000$. We used a 2K Loral CCD detector to register 40 echelle orders partially covering the range from 3500 to 10 000 Å with a length of the spectral orders of about 140 Å at 5500 Å. The polarimeter is located in front of the entrance slit of the spectrograph and consists of a fixed calcite beam splitter aligned along the slit and a rotating super-achromatic quarter-wave plate. Two spectra polarized in opposite sense are recorded simultaneously for each echelle order providing sufficient separation by the cross-dispersion prism below 7000 Å. Two such exposures with the quarter-wave plate angles separated by 90° are necessary to derive circularly polarized spectra. The spectra are usually reduced with the 4A software package (Ilyin 2000). Bias subtraction, master flat-field correction, scattered light subtraction, and weighted extraction of spectral orders comprise the standard steps of the image processing. A ThAr spectral lamp is used for wavelength calibration, taken before and after each target exposure to minimize temporal variations in the spectrograph.

4 Results

The results of our determinations of the mean longitudinal magnetic field $\langle B_z \rangle$ for all studied SPB stars, β Cephei stars, candidate SPB and β Cephei stars, and normal B-type stars are presented in Tables 2a to 2c. In the first two columns we give the HD number and the modified Julian date of the middle of the exposures. The measured mean longitudinal magnetic field $\langle B_z \rangle_{\text{all}}$ using all absorption lines in the Stokes V spectra and $\langle B_z \rangle_{\text{hydr}}$ measured on the hydrogen Balmer lines are presented in Cols. 3 and 4, respectively. As an important step, before the assessment of the longitudinal magnetic field, we excluded all spectral features not belonging to the stellar photospheres of the studied stars: telluric and interstellar features, CCD defects, also emission lines and lines with strong PCygni profiles. For the early-type β Cephei pulsators, a longitudinal magnetic field at a level larger than 3σ has been diagnosed in four β Cephei stars, δ Cet, ξ^1 CMa, HD 50707, and HD 180642, and two stars suspected to be β Cephei stars, HD 74575 and HD 136504. For the SPB stars, a weak magnetic field has been diagnosed in ten SPB stars, HD 3379, HD 24587, HD 25558, HD 28114, HD 28475, HD 74560, HD 85953, HD 140873,

Table 2a The mean longitudinal magnetic field measurements for the β Cephei stars in our sample, observed with FORS 1. In the first two columns we give the HD number and the modified Julian date of the middle of the exposures. The measured mean longitudinal magnetic fields $\langle B_z \rangle$ using all lines or only hydrogen lines are presented in Cols. 3 and 4. All quoted errors are 1σ uncertainties. In Col. 5 we identify new detections by ND and confirmed detections by CD. We note that all claimed detections have a significance of at least 3σ , determined from the formal uncertainties we derive. These measurements are indicated in bold face.

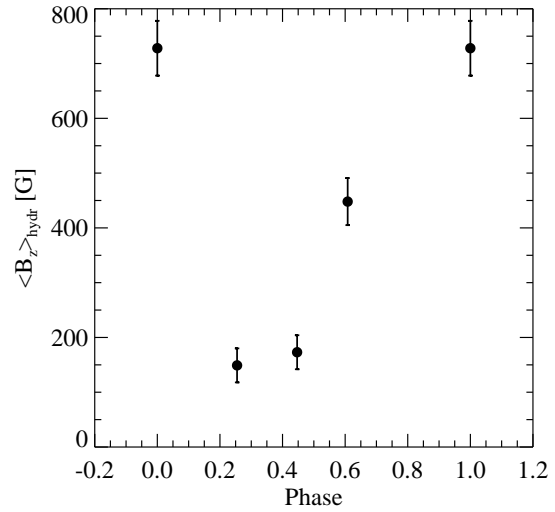
HD	MJD	$\langle B_z \rangle_{\text{all}}$ [G]	$\langle B_z \rangle_{\text{hydr}}$ [G]	Comment
16582	54014.208	-112 ± 36	-142 ± 52	
	54109.066	-88 ± 24	-86 ± 39	
	54040.170	12 ± 31	26 ± 42	
	54047.129	141 ± 83	188 ± 106	
	54343.259	-12 ± 11	-21 ± 15	
	54344.200	-40 ± 12	-75 ± 14	ND
	54344.264	-44 ± 12	-66 ± 21	ND
	54345.203	-42 ± 12	-27 ± 15	
	54345.245	-49 ± 13	-59 ± 15	ND
	54345.293	-31 ± 11	-44 ± 14	ND
29248	54086.286	63 ± 43	66 ± 55	
44743	54046.360	122 ± 52	198 ± 72	
46328	54061.325	369 ± 42	360 ± 45	CD
	54107.266	312 ± 43	319 ± 46	CD
	54114.028	309 ± 35	347 ± 38	CD
	54114.182	364 ± 35	382 ± 47	CD
	54116.108	307 ± 45	276 ± 58	CD
	54155.086	308 ± 47	349 ± 35	CD
	54343.371	345 ± 11	379 ± 15	CD
	54345.338	366 ± 11	400 ± 12	CD
	54345.414	340 ± 11	378 ± 18	CD
	54548.982	324 ± 55	297 ± 87	CD
54549.995	380 ± 37	332 ± 55	CD	
50707	54107.318	163 ± 52	157 ± 58	ND
	54345.372	149 ± 19	123 ± 27	ND
55958	54343.413	-108 ± 45	-97 ± 48	
61068	54107.338	-12 ± 41	-14 ± 45	
74575	54082.341	142 ± 48	-219 ± 60	ND
	54109.150	132 ± 50	184 ± 60	ND
111123	54155.209	107 ± 74	45 ± 86	
	54157.202	95 ± 41	86 ± 50	
129557	54158.229	41 ± 26	77 ± 28	
129929	54177.219	168 ± 59	147 ± 67	
	54343.978	-50 ± 33	-24 ± 41	
132200	54343.995	135 ± 61	175 ± 86	
136504	54344.998	-156 ± 34	-128 ± 36	ND
171034	54344.130	-58 ± 33	-69 ± 37	
172910	54345.176	69 ± 36	72 ± 43	
180642	54343.159	-55 ± 33	-93 ± 38	
	54344.084	166 ± 41	160 ± 55	ND

Table 2b Same as in Table 2a for the observed SPB stars.

HD	MJD	$\langle B_z \rangle_{\text{all}}$ [G]	$\langle B_z \rangle_{\text{hydr}}$ [G]	Comment
3379	54109.048	-53 ± 45	-46 ± 62	
	54112.025	30 ± 28	85 ± 55	
	54344.233	117 ± 34	67 ± 38	CD
	54345.189	155 ± 42	58 ± 52	CD
11462	54344.248	161 ± 46	132 ± 48	ND
23958	54344.397	39 ± 41	9 ± 48	
24587	54086.175	-353 ± 82	-329 ± 91	ND
	54343.301	67 ± 60	83 ± 65	
25558	54086.242	-71 ± 43	-105 ± 48	
	54345.264	105 ± 34	103 ± 41	ND
26326	54086.263	-30 ± 33	-42 ± 60	
26739	54344.283	32 ± 34	39 ± 36	
27742	54345.355	63 ± 42	5 ± 49	
28114	54106.091	107 ± 33	100 ± 44	ND
28475	54107.129	32 ± 38	26 ± 43	
	54345.312	94 ± 36	160 ± 48	ND
29376	54345.279	100 ± 42	77 ± 48	
33331	54344.423	-80 ± 38	-21 ± 42	
34798	54100.150	-99 ± 45	-106 ± 50	
37151	54107.154	-84 ± 40	-68 ± 43	
39844	54344.411	-64 ± 26	-56 ± 28	
40494	54343.426	94 ± 28	39 ± 40	ND
45284	54107.255	-55 ± 50	-64 ± 53	
53921	54061.304	-13 ± 112	-90 ± 117	
55718	54343.401	-2 ± 41	-21 ± 46	
69144	54061.342	-37 ± 52	-64 ± 60	
74195	54108.330	-102 ± 38	-96 ± 43	
74560	54108.348	-198 ± 55	-191 ± 58	CD
85953	54156.096	78 ± 27	97 ± 29	CD
128585	54344.976	112 ± 51	100 ± 57	
140873	54179.299	-144 ± 51	-173 ± 62	
	54344.011	99 ± 31	51 ± 31	CD
152511	54344.116	649 ± 43	728 ± 50	ND
	54608.158	141 ± 26	149 ± 31	ND
	54609.433	440 ± 39	448 ± 43	ND
	54610.223	158 ± 28	173 ± 31	ND
152635	54344.041	-149 ± 36	-167 ± 38	ND
163254	54344.068	155 ± 49	81 ± 60	ND
169467	54345.164	-182 ± 41	-233 ± 43	ND
169820	54345.123	-80 ± 43	-35 ± 48	
179588	54343.134	158 ± 41	184 ± 43	ND
181558	54344.167	-104 ± 32	-103 ± 36	CD
183133	54344.179	152 ± 38	200 ± 43	ND
191295	54343.181	57 ± 38	23 ± 41	
	54345.218	102 ± 36	39 ± 40	
205879	54343.226	150 ± 40	156 ± 43	ND
206540	54344.220	2 ± 27	-5 ± 29	
215573	54042.020	137 ± 52	129 ± 57	
	54343.244	-7 ± 26	-28 ± 29	
	54345.232	66 ± 33	97 ± 38	

Table 2c Same as in Table 2a for the observed normal B stars and the N-rich star HD 52089.

HD	MJD	$\langle B_z \rangle_{\text{all}}$ [G]	$\langle B_z \rangle_{\text{hydr}}$ [G]	Comment
24626	54086.134	10 ± 53	47 ± 59	
52089	54046.339	-200 ± 48	-271 ± 51	ND
	54343.389	-129 ± 34	-156 ± 18	ND
142378	54344.025	129 ± 52	131 ± 62	
153716	54344.057	124 ± 41	113 ± 43	ND
164245	54345.138	116 ± 40	98 ± 46	
166197	54345.153	-69 ± 46	-87 ± 58	
169033	54344.143	77 ± 45	99 ± 48	

**Fig. 1** Longitudinal magnetic field measurements with FORS 1 using hydrogen lines in the candidate SPB star HD 152511 over the period of 0.94 d.

HD 179588, and HD 181558, and eight stars suspected to be SPB, HD 11462, HD 40494, HD 152511, HD 152635, HD 163254, HD 169467, HD 183133, and HD 205879. Out of the ten detections among SPB stars, five are confirmed detections in the stars HD 3379, HD 74560, HD 85953, HD 140873, and HD 181558. These stars have already been studied between 2003 and 2005 and the detected magnetic fields were announced in our previous publication (Hubrig et al. 2006). We could not confirm the presence of magnetic fields at the 3σ level for the previously studied five SPB stars, HD 45284, HD 53921, HD 74195, HD 169820, and HD 215573. These non-detections are likely caused by the strong dependence of the longitudinal magnetic field on rotational aspect. It is generally known that the usefulness of longitudinal magnetic fields in characterizing actual magnetic field strength distributions depends on the sampling of various rotation phases, and hence various aspects of the magnetic field. Among seven normal B-type stars not known as pulsating stars, a weak magnetic field was detected in the nitrogen-rich early B-type star HD 52089 and in the B5 IV star HD 153716.

Among the SPB stars, the detected magnetic fields are mainly of the order of 100–200 G. Only the measurements in HD 24587 revealed the presence of a comparatively large magnetic field of the order of 350 G. For stars observed more than once, the individual measurements show a variability of the magnetic field. However, no exact rotation periods are known for the stars in our sample, and it is certainly not possible with just a few measurements to obtain a clue about the magnetic field geometry causing the observed variations.

A rather strong variable magnetic field has been detected in the candidate SPB star HD 152511 with a maximal field strength of $\langle B_z \rangle_{\text{hydr}} = 728 \pm 50$ G measured on the hydrogen Balmer lines. This star, however, is poorly studied, with only six references in the SIMBAD database. Hipparcos photometric observations reveal a variation period of the order of 0.94 d, which corresponds to the pulsation range of SPB stars. It is presently not clear whether this period is in fact a rotation period and the observed photometric variability could be attributed to an inhomogeneous distribution of chemical elements on the stellar surface. The magnetic field measurements show a positive longitudinal magnetic field over the period of 0.94 d without any change of polarity (Fig. 1). This star obviously deserves future spectropolarimetric, spectroscopic and photometric observations to establish the nature of its variability.

Magnetic fields of the order of several ten to several hundred Gauss have been detected in four β Cephei stars and in two candidate β Cephei stars. The presence of a relatively strong magnetic field in the β Cephei star ξ^1 CMa is confirmed in all eleven measurements carried out since 2005. In Fig. 2 we present our high resolution spectropolarimetric observations with the SOFIN echelle spectrograph at the Nordic Optical Telescope. In spite of rather strong noise, clear Zeeman features are detected at the positions of the unblended lines O II 4676.2 and 4890.9 Å, and He I 5015.7 Å. The latter line is only marginally blended with N II 5016.4 Å. In Fig. 3 we present the acquired measurements of this star over the last 4.4 years with FORS 1. No polarity change is detected in our measurements. Measurements of the magnetic field during the same nights or within one day (MJDs 54114, 54345, 54348–54349) show small changes in the magnetic field strength of the order of a few tens of Gauss, indicating that the field is likely slightly variable on rather short time scales, a couple of days at most. It is not clear yet whether this variability is caused by stellar rotation or by stellar pulsations. On the other hand, from the measured $v \sin i$ value and the radius estimation presented in Table 1a we derive a rotation period in the range from 12 to 33 days. As we reported in our previous study (Hubrig et al. 2006), the radial velocity variability of this star was first discovered by Frost (1907). This star pulsates in a radial mode monoperiodically (Saesen et al. 2006) with a period of 0.209574 d (e.g., Heynderickx et al. 1994). Saesen et al. (2006) found a peak-to-peak radial-velocity amplitude of some 33 km s^{-1} , which is among the largest values ob-

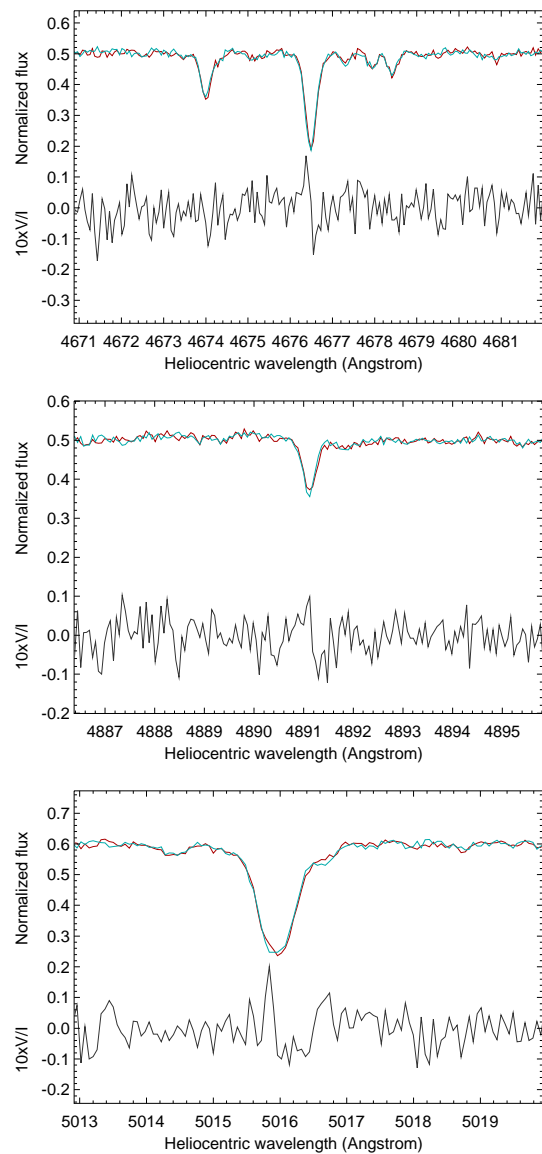


Fig. 2 High-resolution ($R \approx 30\,000$) SOFIN polarimetric spectra of ξ^1 CMa. In each panel, the upper two (blue and red) are the polarized spectra, while the lower spectrum is the deduced V/I spectrum scaled by a factor 10. Clear Zeeman features are detected at the positions of the unblended lines O II 4676.2 and 4890.9 Å. The line He I 5015.7 Å is marginally blended with the N II 5016.4 Å line.

served for a β Cephei star. The amplitude of magnetic field variations is rather low: The obtained values of the longitudinal magnetic fields are in the range from 308 to 380 G for the measurements using all spectral lines and from 276 to 400 G for the measurements using hydrogen lines. Our search for a variation period of the magnetic field in ξ^1 CMa using a Fourier analysis could not reveal any significant frequency.

It is intriguing that the distribution of pulsation periods of early B-type pulsating stars is similar to the distribution of the rotation periods of a number of chemically pecu-

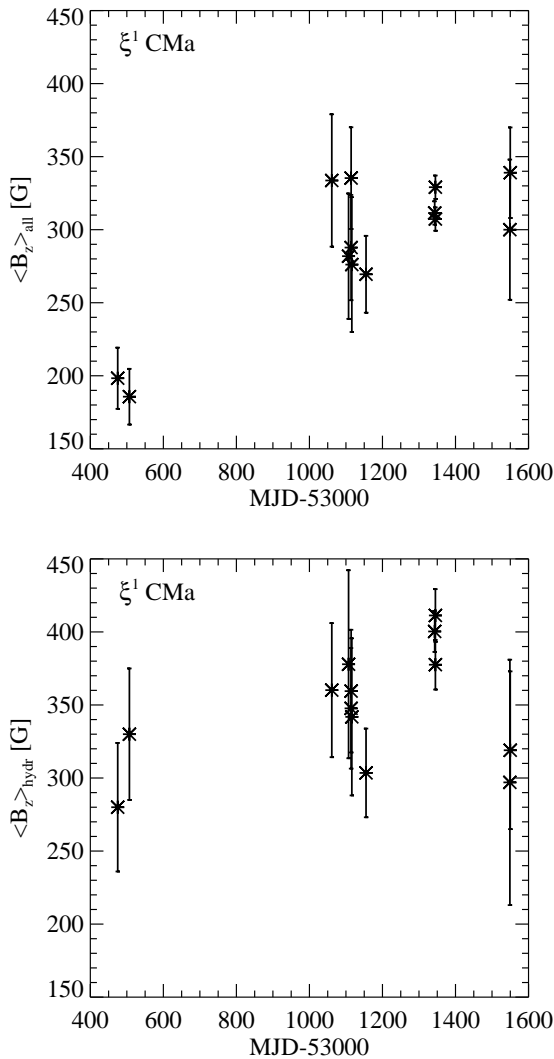


Fig. 3 Magnetic field measurements for ξ^1 CMa in the last 4.4 years, using all lines (*upper panel*) and only the hydrogen lines (*lower panel*).

liar magnetic He-strong stars which occupy approximately the same parameter space in the H-R diagram as β Cephei and SPB stars (e.g., Briquet et al. 2007). The photometric, spectroscopic and magnetic field variations of He-strong stars are usually interpreted in terms of the oblique rotator model. Several such stars, e.g., HD 36485, HD 58260, HD 60344, HD 96446, and HD 133518, with rather short periods, show no polarity change and rather low variability amplitude of the longitudinal magnetic field similar to the magnetic field behaviour of ξ^1 CMa. For the He-strong star HD 96446 Mathys (1994) obtained an unrealistic small radius from the study of the observed magnetic structure, suggesting that the observed variability could be caused by pulsations. Interestingly, all four 3σ magnetic field detections in the β Cephei star δ Cet (Aerts et al. 2006) indicate a negative magnetic field without any change of polarity. According to Aerts et al. (2006), δ Cet is most likely ob-

served nearly pole-on. One more β Cephei star in our sample, HD 50707, does not show any change of polarity either, though only two measurements have been carried out so far for this star.

Recently, Morel et al. (2006, 2008) performed an NLTE abundance analysis of a sample of slowly rotating early-type B dwarfs with detected weak magnetic fields. The studied sample included, among other stars, also a number of SPB and β Cephei stars for which we carried out a magnetic field survey in recent years. This analysis strongly supports the existence of a population of nitrogen-rich and boron-depleted slowly rotating B stars and indicates that the β Cephei stars δ Cet, ξ^1 CMa, HD 50707, and the early B-type star HD 52089 are all nitrogen enriched. For all these stars we have magnetic field detections. In addition, two other β Cephei stars, V2052 Oph and β Cep, of their sample with detected longitudinal magnetic fields of the order of ~ 100 G (Neiner et al. 2003b; Henrichs et al. 2000) were found to show nitrogen enhancement. For the sixth β Cephei star with a detected magnetic field, HD 180642, Morel & Aerts (2007) found a mild nitrogen overabundance, though boron data are not available. Also for the candidate β Cephei star HD 74575 with diagnosed magnetic field, Przybilla et al. (2008) recently detected nitrogen overabundance, while Proffitt & Quigley (2001) found this star to be boron-depleted. Unfortunately, nothing is known about the abundances of these chemical elements for the remaining candidate β Cephei star HD 136504 with a detected magnetic field. In summary, all confirmed and candidate β Cephei stars, with a magnetic field detection and with available N and B abundance values, present a nitrogen enrichment accompanied by a boron depletion.

At present, only for three confirmed and candidate SPBs, all of early B spectral type, is the nitrogen abundance known. Two SPB stars with detected magnetic fields, ζ Cas and HD 85953 have recently been studied by Briquet & Morel (2007). While ζ Cas was found to be nitrogen rich, the analysis of HD 85953 revealed a normal chemical composition. For the candidate SPB star HD 169467, with a measured longitudinal magnetic field $\langle B_z \rangle_{\text{hydr}} = -233 \pm 43$ G, Zboril & North (1999) determined LTE abundance ratios of C, N, and O ($[N/C]$ and $[N/O]$) that are typical of those found by Morel et al. (2008) in their sample of magnetic slowly-rotating B-type dwarfs, indicating that this star is N-rich too. Boesgaard & Heacox (1978) used Copernicus observations to determine the boron abundance in a sample of B-type stars and found HD 169467 to be boron depleted, assigning the same boron abundance to this star as to the magnetic SPB star ζ Cas. The more recent and more reliable analysis of ζ Cas by Proffitt & Quigley (2001) confirmed the very low boron abundance in this magnetic SPB star, and, consequently, that HD 169467 could be boron poor at similar levels. An overview of the available abundance analyses of nitrogen in pulsating B-type stars is given in Table 3, where we present nitrogen over carbon abundance ratios ($[N/C]$). Almost all

Table 3 Logarithmic ratio of the nitrogen and carbon abundances ($[N/C]$) for the β Cephei stars, SPBs and non-pulsating B stars. An asterisk denotes a candidate β Cephei or SPB star, and stars in boldface have a magnetic field detection. The solar $[N/C]$ abundance ratio is about -0.6 dex.

HD	Other Identifier	$[N/C]$ [dex]	Ref.
16582	δ Cet	-0.04 ± 0.14	1
29248	ν Eri	-0.37 ± 0.15	1
44743	β CMa	-0.57 ± 0.18	1
46328	ξ^1 CMa	-0.18 ± 0.21	1
50707	15 CMa	-0.15 ± 0.19	1
61068	PT Pup	-0.15 ± 0.12	2
* 74575	α Pyx	-0.27 ± 0.13	3
111123	β Cru	-0.43 ± 0.20	1
129557	BU Cir	$+0.12 \pm 0.13$	2
129929	V836 Cen	-0.61 ± 0.17	1
180642	V1449 Aql	-0.21 ± 0.22	4
85953	V335 Vel	-0.50 ± 0.24	5
* 169467	α Tel	-0.11 ± 0.20	6
* 215573	ξ Oct	-0.48	7
52089	21 CMa	-0.16 ± 0.19	1

(1) Morel et al. 2008; (2) Kilian 1992; (3) Przybilla et al. 2008; (4) Morel & Aerts 2007; (5) Briquet & Morel 2007; (6) Zboril & North 1999; (7) Pintado & Adelman 2003.

stars with a nitrogen overabundance have detected magnetic fields. Unfortunately, we have only one magnetic field measurement for both HD 61068 and, even more regrettably, HD 129557. The latter is one of the most N-rich B stars known in the solar neighbourhood.

Clearly, the presently available observational data suggest a higher incidence of chemical peculiarities in stars with detected magnetic fields. We note that δ Cet, HD 50707, and HD 52089 have been included in this survey primarily because they were nitrogen rich. These results open a new perspective for the selection of the most promising targets for magnetic field surveys of massive stars using chemical anomalies as selection criteria.

5 Discussion

Out of 13 β Cephei stars studied to date with FORS 1, four stars (31%) possess weak magnetic fields, and out of the sample of six suspected β Cephei stars two stars show a weak magnetic field. The fraction of magnetic SPBs and candidate SPBs is found to be higher: roughly half of the 34 SPB stars (53%) were found to be magnetic and among the 16 candidate SPBs eight stars (50%) possess magnetic fields. In an attempt to understand why only a fraction of pulsating stars exhibit magnetic fields, we studied the position of magnetic and non-magnetic pulsating stars in the H-R diagram. Their distribution is shown in Fig. 4. In this figure filled circles correspond to confirmed SPB stars, open circles to candidate SPB stars, filled stars to confirmed β Cephei stars, open stars to candidates β Cephei stars, and squares to standard B stars. The stars with detected magnetic fields are presented by symbols which are 1.5 times bigger than those for stars for which magnetic fields were not detected. The instability strips shown in Fig. 4 were determined from theoretical models for main-sequence stars with $2 \leq M/M_{\odot} \leq 15$. For these models, the instability of the modes with $\ell \leq 3$ and eigenfrequencies between 0.2 and 25 d^{-1} was checked. The hence derived instability strips only contain models having unstable β Cephei- and/or SPB-like modes (De Cat et al. 2007). From the locations of the boundaries of the instability strips it is clear that β Cephei stars are not found close to the ZAMS as they are not predicted to be there. Some concentration of less massive SPB stars towards the ZAMS is in agreement with expectations from evolutionary models, as the evolution time near the TAMS is faster than the evolution time close to the ZAMS. For hotter SPBs there are only unstable modes in the stars close to the TAMS. The magnetic SPB stars with masses $\leq 4 M_{\odot}$ seem to be concentrated closer to the ZAMS than the higher mass stars. On the other hand, no clear picture emerges as to the possible evolution of the magnetic field across the main sequence. Among the most massive β Cep stars, two magnetic stars, ξ^1 CMa and HD 50707, are located close to the boundary of the theoretical instability strip. δ Cet with the weakest magnetic field detected in our

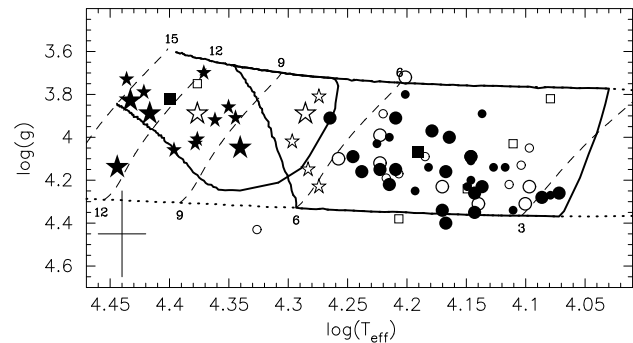


Fig. 4 The position of the studied pulsating and non-pulsating stars in the H-R diagram. The sample includes all targets for which FORS 1 spectropolarimetric observations are available (this study and Hubrig et al. 2006). The full lines represent the boundaries of the theoretical instability strips for modes with frequencies between 0.2 and 25 d^{-1} and $\ell \leq 3$, computed for main-sequence models with $2 \leq M/M_{\odot} \leq 15$ (De Cat et al. 2007). The lower and upper dotted lines show the zero-age main sequence and terminal-age main sequence, respectively. The dashed lines denote evolution tracks for stars with $M = 15, 12, 9, 6,$ and $3 M_{\odot}$. Filled circles correspond to confirmed SPB stars, open circles to candidate SPB stars, filled stars to confirmed β Cephei stars, open stars to candidates β Cephei stars, and squares to standard B stars. The stars with detected magnetic fields are presented by symbols which are 1.5 times bigger than those for stars for which magnetic fields were not detected. The cross in the bottom left corner gives the typical error estimate, 0.02 on $\log T_{\text{eff}}$ and 0.2 on $\log g$. The parameters of objects with $M > 12 M_{\odot}$ are less reliable because these values were found by extrapolation out of the calibration tables.

β Cephei stars, open stars to candidates β Cephei stars, and squares to standard B stars. The stars with detected magnetic fields are presented by symbols which are 1.5 times bigger than those for stars for which magnetic fields were not detected. The instability strips shown in Fig. 4 were determined from theoretical models for main-sequence stars with $2 \leq M/M_{\odot} \leq 15$. For these models, the instability of the modes with $\ell \leq 3$ and eigenfrequencies between 0.2 and 25 d^{-1} was checked. The hence derived instability strips only contain models having unstable β Cephei- and/or SPB-like modes (De Cat et al. 2007). From the locations of the boundaries of the instability strips it is clear that β Cephei stars are not found close to the ZAMS as they are not predicted to be there. Some concentration of less massive SPB stars towards the ZAMS is in agreement with expectations from evolutionary models, as the evolution time near the TAMS is faster than the evolution time close to the ZAMS. For hotter SPBs there are only unstable modes in the stars close to the TAMS. The magnetic SPB stars with masses $\leq 4 M_{\odot}$ seem to be concentrated closer to the ZAMS than the higher mass stars. On the other hand, no clear picture emerges as to the possible evolution of the magnetic field across the main sequence. Among the most massive β Cep stars, two magnetic stars, ξ^1 CMa and HD 50707, are located close to the boundary of the theoretical instability strip. δ Cet with the weakest magnetic field detected in our

Table 4 The frequencies and the corresponding photometric pulsating amplitudes of all pulsating stars for which magnetic fields have been detected with FORS 1. An asterisk denotes candidate β Cep and SPB stars.

HD	f_1 [c/d]	a_1 [mmag]	f_2 [c/d]	a_2 [mmag]	f_3 [c/d]	a_3 [mmag]	f_4 [c/d]	a_4 [mmag]
	f_5 [c/d]	a_5 [mmag]	f_6 [c/d]	a_6 [mmag]	f_7 [c/d]	a_7 [mmag]	f_8 [c/d]	a_8 [mmag]
β Cep stars								
16582	6.20589(M)	11.6	3.737(M)	0.53	3.672(M)	0.39	0.318(M)	0.68
46328	4.77153(GHSp)	32.4						
* 50707	5.4187(GHStSp)	6.2	5.1831(St)	5.4	5.5212(St)	2.0	5.3085(St)	1.6
* 136504	10.36(Sp)							
180642	5.4869(G)	82.8	0.3082(G)	5.2	7.3667(G)	4.6		
SPB stars								
3379	1.82023(G)	5.0	1.59418(G)	4.2				
* 11462	1.33482(H)	18.0	1.44486(H)	12.0				
24587	1.1569(GHSp)	13.1						
25558	0.65265(GH)	26.3	1.93235(GH)	6.2	1.17913(G)	5.1		
28114	0.48790(G)	26.2	0.48666(G)	12.9	0.79104(H)			
28475	0.68369(GH)	14.9	0.40893(G)	8.8				
45284	1.23852(G)	13.3	1.12753(G)	19.5	1.50605(G)	9.1	1.32975(H)	9.7
53921	0.6054(GHSp)	12.8						
74195	0.35745(GHSp)	23.4	0.35033(GHSp)	18.8	0.34630(GHSp)	6.0	0.39864(GHSp)	4.5
74560	0.64472(GHSp)	25.0	0.39578(G Sp)	7.0	0.44763(G)	6.0	0.82281(GH)	5.4
	0.63567(GH)	5.7						
85953	0.2663(GHSp)	14.7	0.2189(GH)	5.1	0.2353(Sp)			
140873	1.1515(GHSp)	28.4						
* 152511	1.0614(H)	14.3						
* 152635	0.5211(H)	20.4						
160124	0.52014(G)	23.7	0.52096(G)	18.9	0.52055(G)	23.5	0.52137(G)	20.1
	0.52197(G)	22.3	0.70259(G)	15.0	1.04220(G)	10.7	0.31366(G)	11.5
161783	0.7351(St)	6.5	0.5602(St)	6.2	0.9254(St)	3.0	0.3256(St)	4.8
* 163254	1.20241(H)	24.9						
* 169467	1.1003(H)	6.2						
169820	2.12509(GH)	13.6						
179588	0.85654(G)	29.7	2.04263(G)	17.6	2.19989(G)	16.2	1.83359(G)	13.5
	0.81599(H)	18.4						
181558	0.80780(GHSp)	49.5						
* 183133	0.98177(H)	16.9						
* 205879	1.01729(H)	20.0	0.98251(H)	8.0				
208057	0.89050(GH)	13.5	0.80213(GH)	9.4	2.47585(G)	9.1		
* 215573	0.5439(H)	11.5	0.5654(GHSp)	10.8				

(G) – Geneva photometry; (H) – Hipparcos photometry; (M) – MOST Photometry; (Sp) – Spectroscopic data; (St) – Stromgren photometry.

sample of β Cep stars is also the least massive target of this group and is located close to the center of the main sequence. The fourth β Cep star with a detected magnetic field, HD 180642, might be the youngest object in our β Cep star sample, but the parameters are not very reliable (see Sect. 2). From the position of magnetic and non-magnetic pulsating stars, including also the two normal B-type stars, HD 153716 and the nitrogen rich star HD 52089, it is obvious that their domains in the H-R diagram largely overlap. For this reason we suggest that the evolutionary age cannot be the decisive factor for the presence of a magnetic field in

pulsating stars. This suggestion is also supported by Fig. 5 where we present the strength of the longitudinal magnetic field measured in confirmed pulsating β Cep and SPB stars and candidate β Cep and SPB stars as a function of the completed fraction of the main-sequence lifetime. In this figure and all subsequent figures, we use the data from this study and from Hubrig et al. (2006). The magnetic field strength is used in absolute values, without taking into account the polarity of the field. No obvious trend for the change of the strength of the magnetic field across the H-R diagram can be detected. We also find no trend between the distribution of

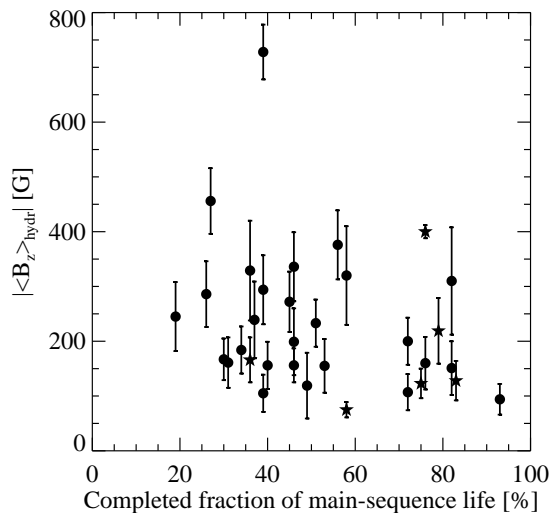


Fig. 5 The strength of the longitudinal magnetic field measured with FORS 1 using hydrogen lines as a function of the completed fraction of the main-sequence lifetime. Filled stars indicate β Cephei stars and candidate β Cephei stars, while filled circles indicate SPBs and candidate SPBs.

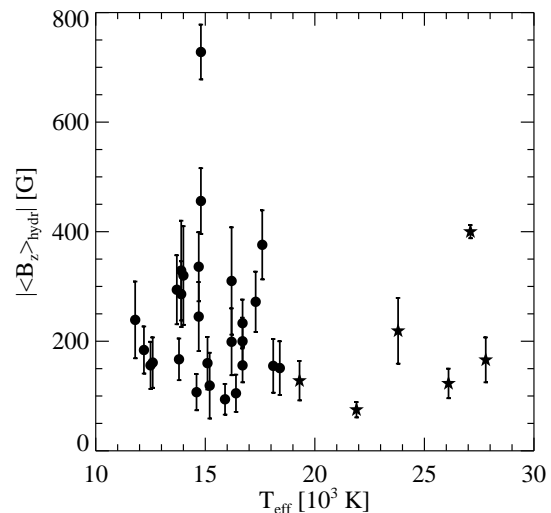


Fig. 7 The strength of the longitudinal magnetic field measured with FORS 1 using hydrogen lines as a function of effective temperature. The symbols are identical to those presented in Fig. 5.

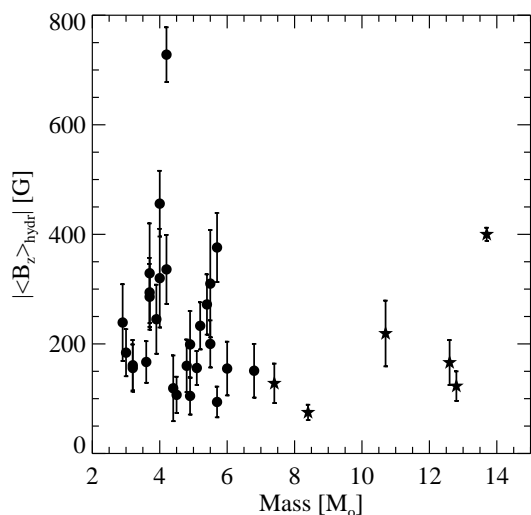


Fig. 6 The strength of the longitudinal magnetic field measured with FORS 1 using hydrogen lines as a function of stellar mass. The symbols are identical to those presented in Fig. 5.

the strength of the magnetic field and stellar mass or effective temperature, though for the small sample of β Cephei stars a slight increase of the strength of the magnetic field with the stellar mass and effective temperature is possible (Figs. 6 and 7).

In Table 4 we present the frequencies and the corresponding pulsating amplitudes of all pulsating stars for which magnetic fields have been detected with FORS 1 up to now. For the candidate β Cephei star HD 136504 no amplitude is given since only spectroscopic observations have been carried out. As we already mentioned in Sect. 2, four

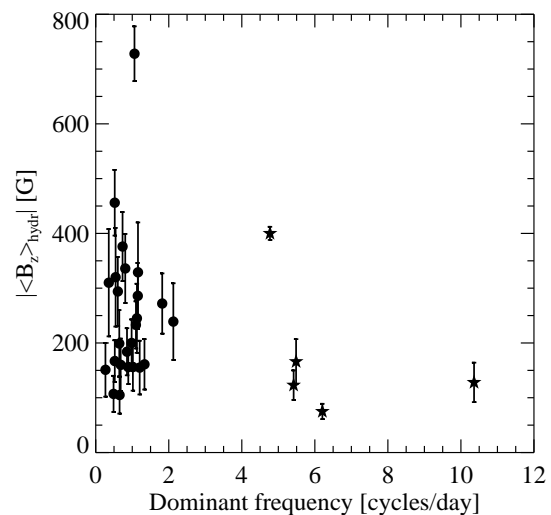


Fig. 8 The strength of the longitudinal magnetic field measured with FORS 1 using hydrogen lines as a function of frequency presented in Table 4. For multiperiodic stars we selected the pulsation mode with the highest amplitude. The symbols are identical to those in Fig. 5.

magnetic β Cephei stars, δ Cet, ξ^1 CMa, V2052 Oph, and β Cep have another common property: they are either radial pulsators (ξ^1 CMa) or their pulsations are dominated by a radial mode (δ Cet, β Cep, and V2052 Oph). In addition, Aerts (2000) found HD 180642 to be a large amplitude non-linear pulsator with a dominant radial mode. Although the mode identification for the main frequency of the β Cephei star HD 50707 is not completely clear, it has been shown by other authors that this star pulsates non-linearly (Shobbrook et al. 2006; Heynderickx 1992) as is the case for all magnetic β Cephei stars for which the pulsational behaviour has

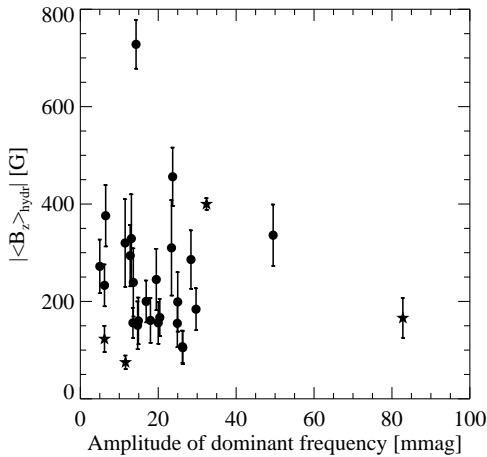


Fig. 9 The strength of the longitudinal magnetic field measured with FORS 1 using hydrogen lines as a function of the pulsation amplitude of the dominant frequency. The symbols are identical to those presented in Fig. 5.

been carefully studied in the past. It is therefore quite possible that there might be a link between such a non-linear pulsation behaviour dominated by a radial mode and the presence of a magnetic field.

In Figs. 8 and 9 we plot the strength of the magnetic field as a function of the pulsation frequency and the corresponding pulsating amplitudes. For multiperiodic stars we use in Fig. 8 the frequency of the pulsation period with the highest amplitude. It is possible that stronger fields tend to be found in stars with lower pulsating frequencies and smaller pulsating amplitudes.

In Fig. 10 we display the strength of the magnetic field as a function of $v \sin i$ -values. The majority of pulsating stars have rather low $v \sin i$ -values, less than 30 km s^{-1} , and it is possible that the magnetic stars are rotating more slowly. Magnetic braking and angular momentum transport along the field lines would offer a natural explanation for the slow rotation of our magnetic pulsating stars. Slow rotation is one of the main characteristics of Ap and Bp stars and it is generally assumed that Ap stars are slow rotators because of magnetic braking. However, this judgment about the slow rotation of pulsating stars is based on the assumption that the stars with the low $v \sin i$ -values are not actually viewed pole-on stars. On the other hand, considering random inclination angles and the size of our sample, the number of pole-on stars should be rather small. For no star is the rotation period known to date. The rotation periods of pulsating stars can currently be rather easily determined by space-based monitoring with the up-coming mission of the nanosatellites BRITE (BRiGht Target Explorer) or with the already in orbit microsatellite MOST (Microvariability and Oscillations of STars). These satellites can provide intense photometric monitoring to search and precisely identify pulsation modes and rotationally split modes in both, SPB and β Cep stars, and in Bp stars (we refer to Sect. 4 with the discussion related to He-strong stars). Such observations will

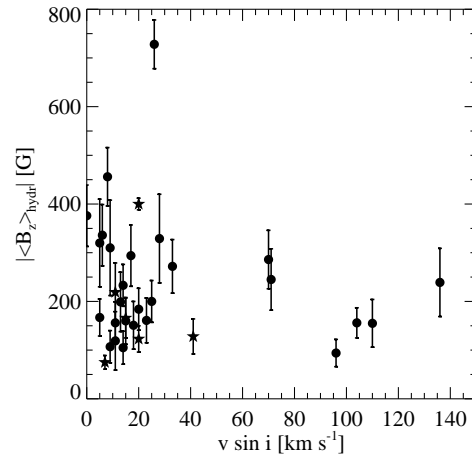


Fig. 10 The strength of the longitudinal magnetic field measured with FORS 1 using hydrogen lines as a function of $v \sin i$. The symbols are identical to those presented in Fig. 5.

be crucial for the understanding of the generation mechanism of the magnetic field in hot B-type stars.

In summary, we have demonstrated that a significant fraction of pulsating B stars are magnetic. This is a very important result, which should be included in future discussions related to theoretical works similar to that of Hasan et al. (2005). The presented magnetic field measurements in pulsating stars confirm that their longitudinal magnetic fields are rather weak in comparison to the kG fields detected in magnetic Bp stars. Although our results provide some new clues, the observational results presented in this work are still inconclusive as to the difference between magnetic and non-magnetic pulsating stars. The present-day magnetic field data are far from sufficient to prove the existence of either pulsational or rotational variability of magnetic fields in the studied stars. Additional future magnetic field measurements are also needed to study the indicated loose trends in the few dependencies presented above. Abundance studies of nitrogen and boron in B-type stars are still scarce. It will be important to carry out sophisticated abundance analyses for all pulsating stars. Besides confirming the use of the chemical anomaly as an indicator for the presence of magnetic fields, it will also be of importance to obtain abundances for pulsating stars with non-detections. Such analyses are necessary to convincingly reveal a dichotomy between the two groups.

Acknowledgements. MB is Postdoctoral Fellow of the Fund for Scientific Research, Flanders. We would like to thank to H.F. Henrichs for valuable comments. This research has made use of the SIMBAD database, operated at CDS, Strasbourg, France.

References

- Abt, H.A., Levato, H., Grosso, M.: 2002, ApJ 573, 359
- Aerts, C.: 2000, A&A 361, 245
- Aerts, C., De Cat, P., Cuypers, J.: 1998, A&A 329, 137
- Aerts, C., De Cat, P., Handler, G., et al.: 2004a, MNRAS 347, 463

- Aerts, C., Waelkens, C., Daszyńska-Daszkiewicz, J., et al.: 2004b, A&A 415, 241
- Aerts, C., Marchenko, S.V., Matthews, J.M., et al.: 2006, ApJ 642, 470
- Balona, L.A.: 1975, MmRAS 78, 51
- Boesgaard, A.M., Heacox, W.D.: 1978, ApJ 226, 888
- Briquet, M., Morel, T.: 2007, CoAst 150, 183
- Briquet, M., De Cat, P., Aerts, C., Scuflaire, R.: 2001, A&A 380, 177
- Briquet, M., Aerts, C., Lüftinger, T., et al.: 2004, A&A 413, 273
- Briquet, M., Hubrig, S., De Cat, P., et al.: 2007, A&A 466, 269
- De Cat, P., Aerts, C.: 2002, A&A 393, 965
- De Cat, P., Briquet, M., Aerts, C., et al.: 2006, CoAst 147, 48
- De Cat, P.: 2007, CoAst 150, 167
- De Cat, P., Briquet, M., Aerts, C., et al.: 2007, A&A 463, 243
- Frost, E.B.: 1907, ApJ 25, 59
- Hasan, S.S., Zahn, J.-P., Christensen-Dalsgaard, J.: 2005, A&A 444, L29
- Hempel, M., Holweger, H.: 2003, A&A 408, 1065
- Henrichs, H.F., Neiner, C., Hubert, A.M., et al.: 2000, in: M.A. Smith, H.F. Henrichs (eds.), *The Be Phenomenon in Early-Type Stars*, ASPC 214, p. 372
- Heynderickx, D.: 1992, A&AS 96, 207
- Heynderickx, D., Waelkens, C., Smeyers, P.: 1994, A&AS 105, 447
- Hubrig, S., Kurtz, D.W., Bagnulo, S., et al.: 2004a, A&A 415, 661
- Hubrig, S., Szeifert, T., Schöller, M., et al.: 2004b, A&A 415, 685
- Hubrig, S., Briquet, M., Schöller, M., et al.: 2006, MNRAS 369, L61
- Ilyin, I.: 2000, PhD Thesis, University of Oulu, Finland
- Kilian, J.: 1992, A&A 262, 171
- Künzli, M., North, P., Kurucz, R.L., Nicolet, B.: 1997, A&AS 122, 51
- Mathias, P., Aerts, C., Briquet, M., et al.: 2001, A&A 379, 905
- Mathys, G.: 1994, in: L.A. Balona, H.F. Henrichs, J.M. Le Contel (eds.), *Pulsation, Rotation, and Mass Loss in Early-Type Stars*, IAU Symp. 162, p. 169
- Morel, T., Aerts, C.: 2007, CoAst 150, 201
- Morel, T., Butler, K., Aerts, C., et al.: 2006, A&A 457, 651
- Morel, T., Hubrig, S., Briquet, M.: 2008, A&A 481, 453
- Neiner, C., Geers, V.C., Henrichs, H.F., et al.: 2003a, A&A 406, 1019
- Neiner, C., Henrichs, H.F., Floquet, M., et al.: 2003b, A&A 411, 565
- Pintado, O.I., Adelman, S.J.: 2003, A&A 406, 987
- Proffitt, C.R., Quigley, M.F.: 2001, ApJ 548, 429
- Przybilla, N., Nieva, M.F., Heber, U., et al.: 2008, A&A 480, L37
- Royer, F., Grenier, S., Baylac, M.-O., et al.: 2002, A&A 393, 897
- Saesen, S., Briquet, M., Aerts, C.: 2006, CoAst 147, 109
- Scuflaire, R., Théado, S., Montalbán, J., et al.: 2008, Ap&SS 316, 83
- Shobbrook, R.R., Handler, G., Lorenz, D., Mogorosi, D.: 2006, MNRAS 369, 171
- Tuominen, I., Ilyin, I., Petrov, P.: 1999, in: H. Karttunen, V. Pirola (eds.), *Astrophysics with the NOT*, p. 47
- Uytterhoeven, K., Aerts, C., De Cat, P., et al.: 2001, A&A 371, 1035
- Waelkens, C., Aerts, C., Kestens, E., et al.: 1998, A&A 330, 215
- Zboril, M., North, P.: 1999, A&A 345, 244